Received: 20 May 2020 | Revised: 3 September 2020 | Accepted: 14 September 2020

DOI: 10.1002/tox.23034

RESEARCH ARTICLE

ENVIRONMENTAL TOXICOLOGY WILEY

Poly(ADP-ribose) glycohydrolase silencing-mediated H2B expression inhibits benzo(a)pyrene-induced carcinogenesis

Zhuoying Zeng[1,2] | Jingjing Lu[3] | Desheng Wu[4] | Ran Zuo[3] | Yuxi Li[3,5] | Haiyan Huang[4] | Jianhui Yuan[3] | Zhangli Hu[1,2]

[1]College of Life Sciences and Oceanography, Shenzhen University, Shenzhen, China

[2]College of Physics and Optoelectronic Engineering, Shenzhen University, Shenzhen, China

[3]Nanshan District Center for Disease Control and Prevention, Shenzhen, China

[4]Shenzhen Center for Disease Control and Prevention, Shenzhen, China

[5]Xiangya School of Public Health, Central South University, Changsha, China

Correspondence
Zhangli Hu, College of Life Sciences and Oceanography, Shenzhen University, Shenzhen 518060, China.
Email: huzl@szu.edu.cn

Jianhui Yuan, Nanshan District Center for Disease Control and Prevention, Shenzhen 518054, China.
Email: jianhui_yuan@126.com

Haiyan Huang, Shenzhen Center for Disease Control and Prevention, Shenzhen 518055, China.
Email: hhy424@126.com

Funding information
Guangdong Medical Science and Technology Research Fund, Grant/Award Number: A2019554; Guangdong natural science foundation general project, Grant/Award Number: 2019A1515011080; Shenzhen basic research discipline layout project, Grant/Award Number: JCYJ20160328161613864; Shenzhen Basic Research Project, Grant/Award Number: JCYJ20190807102803567

Abstract

Poly(ADP-ribose) glycohydrolase (PARG) as a main enzyme hydrolyzing poly(ADP-ribose) in eukaryotes, and its silencing can inhibit benzo(a)pyrene (BaP)-induced carcinogenesis. A thorough understanding of the mechanism of *PARG* silenced inhibition of BaP-induced carcinogenesis provides a new therapeutic target for the prevention and treatment of environmental hazard induced lung cancer. We found that the expression of several subtypes of the histone H2B was downregulated in BaP-induced carcinogenesis via *PARG* silencing as determined by label-free proteomics and confirmed by previous cell line- and mouse model-based studies. Analysis using the GEPIA2 online tool indicated that the transcription levels of *H2BFS*, *HIST1H2BD*, and *HIST1H2BK* in lung adenocarcinoma (LUAD) tissues and squamous cell lung carcinoma (LUSC) tissues were higher than those in normal lung tissues, while the transcription levels of *HIST1H2BH* in LUSC tissues were higher than those in normal lung tissues. The expression levels of *HIST1H2BB*, *HIST1H2BH*, and *HIST1H2BL* were significantly different in different lung cancer (LC) stages. Moreover, the expression of *H2BFS*, *HIST1H2BD*, *HIST1H2BJ*, *HIST1H2BK*, *HIST1H2BL*, *HIST1H2BO*, *HIST2H2BE*, and *HIST2H2BF* was positively correlated with that of *PARG* in LC tissues. Analysis of the Kaplan-Meier plotter database indicated that high H2B levels predicted low survival in all LC patients suggesting that H2B could be a new biomarker for determining the prognosis of the LC, and that its expression can be inhibited by *PARG* silencing in BaP-induced carcinogenesis.

KEYWORDS

benzo(a)pyrene, lung cancer, poly(ADP-ribose) glycohydrolase, tumorigenesis

1 | INTRODUCTION

Poly(ADP-ribose) glycohydrolase (PARG) is the main enzyme that hydrolyzes poly(ADP-ribose) in eukaryotes and plays an important role in tumorigenesis.[1,2] In our previous study, *PARG* silencing inhibited the malignant transformation induced by benzo(a)pyrene (BaP), but its mechanism was unclear.[3,4]

The histone H2B and its subtypes perform diverse biological functions, and their expression levels vary among different types of cancer. *HIST1H2BA* (H2B type 1-A) maintains the integrity of testicular specific proteins and chromatin.[5] *HIST1H2BJ* (H2B type 1-J) is involved in chromatin remodeling in schizophrenia.[6] *HITT2H2BE* (H2B type 2-E) inhibits cell proliferation and deactivates odor sensing neurons.[7,8] Another study reported that *HIST1H2BG*, *HIST1H2BJ*, *HIST2H2BE*, *HIST1H2BC*, *HIST1H2BH*, and *HIST1H2BE* are highly expressed in lung adenocarcinoma (LUAD) tissues.[9] Several similar studies have shown that H2B are highly expressed in lung cancer (LC) tissues. All the above mentioned evidence indicates that H2B plays an important role in lung tumorigenesis, but its regulatory mechanism is still unknown.

In our previous study, *PARG* silencing effectively prevented the development of BaP-induced LC. In this study, we found that *PARG* silencing prevents the development of BaP-induced LC by stabilizing the abnormally high levels of H2B, which plays an important role in the staging and prognosis of LC. Our results provide strong evidence for elucidating the LC development. Different H2B subtypes exhibit different protein structures and sequences, indicating that they undergo different chemical modifications. Histone posttranslational modifications represent a diverse set of epigenetic marks that are involved, not only in dynamic cellular processes, such as transcription and DNA repair, but also in destabilizing chromatin.[10-12] The mechanism elucidated in the present study will provides a strong basis for future studies on the role of H2B-modified pedigree expression in lung tumorigenesis.

2 | MATERIALS AND METHODS

2.1 | Cell lines and culture selection

The cell lines used in this study was been constructed in our previous work.[4] The normal human bronchial epithelial cell line (C-16HBE cells) and human bronchial epithelial cells with a silenced *PARG* gene (C-shPARG cells) were used as the control groups and were grown in minimum essential Eagle's medium (Gibco, The United States) containing 10% fetal bovine serum (Gibco, The United States). BTC-16HBE and BTC-shPARG cells were treated with 40 μM BaP (Sigma, The United States) 1 day/week for 15 weeks.

2.2 | Mouse model establishment

The mouse model used in this study was constructed in our previous work.[13] Wild-type C57 mice with malignant transformation induced by BaP (C57-female-T) and mice with silenced *PARG* gene without malignant transformation under the same treatment conditions (shPARG-female-T) were used. C57-female-C and shPARG-female-C mouse models without BaP treatment were used as the control groups.

Treatment and maintenance of animals were performed according to the regulations of the Animal Care and Use Committee of Shenzhen CDC Experimental Animal Center. The mice were anesthetized with ether prior to experimentation, and we followed all the necessary procedures to ensure that no unnecessary pain was inflicted at any stage of the experiment.

2.3 | Label-free proteomics

An acid extraction assay was performed for histones extraction.[14] The products digested by arginase (Arg-C) were separated by high-performance liquid chromatography, and raw data were analyzed using Q Exactive. The raw data were analyzed using the human protein sequence database SwissProt. The software Proteome Discoverer (Thermo, The United States) was used for data comparison to obtain qualitative and quantitative information of protein or peptide segments in each group. Quantitative information was analyzed using the Perseus software.

2.4 | Western blotting

Western blotting experiment based on the previous articles.[13] The relative expression of H2B (Abcam, England) was assessed relative to that of β-actin (Santa Cruz, The United States). Histogram construction and statistical analysis of the relative expression of each group were performed using the GraphPad Prism software and Student's *t* test.

2.5 | Immunofluorescence

Immunofluorescence analysis was performed according to a method described previously.[13]

2.6 | Bioinformatics analysis

GEPIA2 (http://gepia2.cancer-pku.cn/#index) was used to analyze the relative expression of H2B subtypes and their relationship with tumor stage in LC patients. The log2(TPM) was calculated simply as log2 of the transcript count per million (TPM) and log2FC was calculated as median (Tumor) − median (Normal). TPM is a normalization technique to scale the read count per gene/transcript toward the total read count of the sequencing run to compensate for different sequencing depths. The expression data were first transformed into long2(TPM + 1) values for differential analysis. Genes with higher |log2FC|

values and lower *q* values than pre-set thresholds were considered to be differentially expressed. Differential gene expression was analyzed using one-way analysis of variance by considering the pathological stage as a variable. GEPIA2 was also used for performing gene correlation analysis (Pearson analysis) of PARG and H2B subtypes in LC. We used nonlog-scale axis for calculation, and the log-scale axis for visualization. Kaplan-Meier Plotter (www.kmplot.com) was used to analyze the relationship between the H2B subtype and overall survival (OS), progression-free survival (FP), and progressive postpartum survival (PPS) in LC patients.

3 | RESULT

3.1 | Label-free proteomics explains the inhibition of the abnormal increase in the H2B level by *PARG* silencing in BaP-induced carcinogenesis

Label-free proteomics was used to determine the expression of histone subtypes in 16HBE and shPARG cells with or without BaP treatment. The results suggested that the relative expression of H2B subtypes increased in BTC-16HBE cells but remained unchanged in BTC-shPARG cells (Table 1 and Figure 1).

TABLE 1 Histone expression level analyzed by proteomics

Group	Gene	Description	Fold change	*P*-value
BTC-16HBE/C-16HBE	H1FV	Histone H1.0	−1.11	.03
BTC-16HBE/C-16HBE	HIST1H1E	Histone H1.4	−0.87	.01
BTC-16HBE/C-16HBE	HIST2H2AC	Histone H2A type 2-C	1.27	.01
BTC-16HBE/C-16HBE	H2BFS	Histone H2B type F-S	6.14	<.01
BTC-16HBE/C-16HBE	HIST1H2BB	Histone H2B type 1-B	5.41	<.01
BTC-16HBE/C-16HBE	HIST1H2BC	Histone H2B type 1-C/E/F/G/I	5.39	.01
BTC-16HBE/C-16HBE	HIST1H2BD	Histone H2B type 1-D	4.87	<.01
BTC-16HBE/C-16HBE	HIST1H2BH	Histone H2B type 1-H	4.9	<.01
BTC-16HBE/C-16HBE	HIST1H2BJ	Histone H2B type 1-J	6.29	<.01
BTC-16HBE/C-16HBE	HIST1H2BK	Histone H2B type 1-K	5.86	<.01
BTC-16HBE/C-16HBE	HIST1H2BL	Histone H2B type 1-L	5.61	<.01
BTC-16HBE/C-16HBE	HIST1H2BM	Histone H2B type 1-M	4.21	.03
BTC-16HBE/C-16HBE	HIST1H2BO	Histone H2B type 1-O	5.43	<.01
BTC-16HBE/C-16HBE	HIST2H2BE	Histone H2B type 2-E	4.57	.01
BTC-16HBE/C-16HBE	HIST2H2BF	Histone H2B type 2-F	4.92	.01
BTC-16HBE/C-16HBE	HIST1H3A	Histone H3.1	−2.03	<.001
BTC-16HBE/C-16HBE	HIST3H3	Histone H3.1t	−1.77	<.001
BTC-16HBE/C-16HBE	HIST2H3A	Histone H3.2	−2.03	<.001
BTC-16HBE/C-16HBE	H3F3C	Histone H3.3C	−1.94	<.001
BTC-shPARG/C-shPARG	HIST2H2AC	Histone H2A type 2-C	1.11	.42

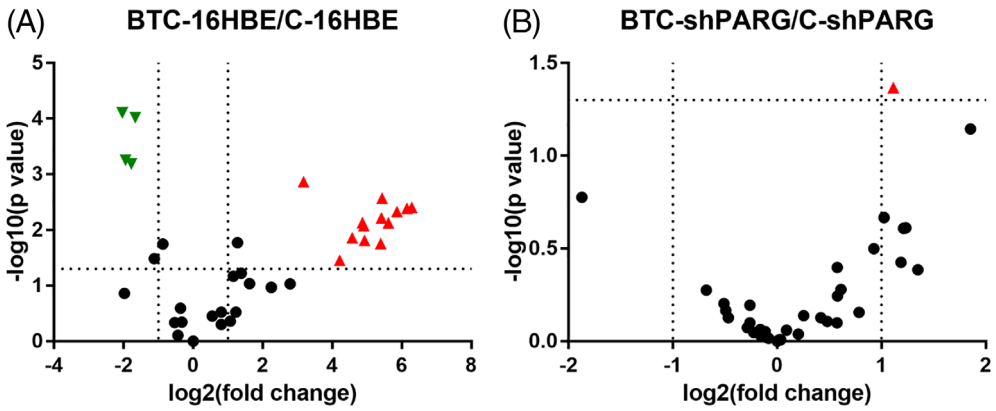

FIGURE 1 *PARG* silencing down-regulates H2B levels in BaP-induced carcinogenesis. A, A volcano plot showing histone expression in BTC-16HBE/C-16HBE. B, A volcano plot showing histone expression in BTC-shPARG/C-shPARG. The red equilateral triangle represents the protein with significantly high expression, while the green inverted triangle represents the protein with significantly low expression [Color figure can be viewed at wileyonlinelibrary.com]

3.2 | PARG silencing-mediated downregulation of H2B expression in BaP-induced carcinogenesis was confirmed in cell lines and mouse models

Western blotting results indicated that the relative expression of H2B in BTC-16HBE cells was higher than that in C-16HBE cells (mean ± SD = 0.5542 ± 0.1482, P = .0038), while the relative expression of H2B in BTC-shPARG cells was lower than in C-shPARG cells (mean ± SD = −1.157 ± 0.3553, P = .0087) (Figure 2A,B). An increase in H2B fluorescence intensity was observed in BTC-16HBE cells compared with that in C-16HBE cells, that no significant difference in the H2B fluorescence intensity was observed in BTC-shPARG cells compared with that in C-shPARG cells (Figure 2E). In addition, in vivo studies showed an increase in the relative expression of H2B in C57-Female-T mice compared with that in C57-Female-C mice (mean ± SD = 0.2747 ± 0.02173, P < .0001), and a decrease in the relative expression of H2B in shPARG-Female-T mice compared with that in shPARG-Female-C mice (mean ± SD = −0.07096 ± 0.02788, P = .0438) (Figure 2C,D).

3.3 | Relationship between the mRNA levels of H2B and LC

We compared the mRNA expression of H2B in LC tissues with that in normal lung tissues using the GEPIA2 dataset. The results

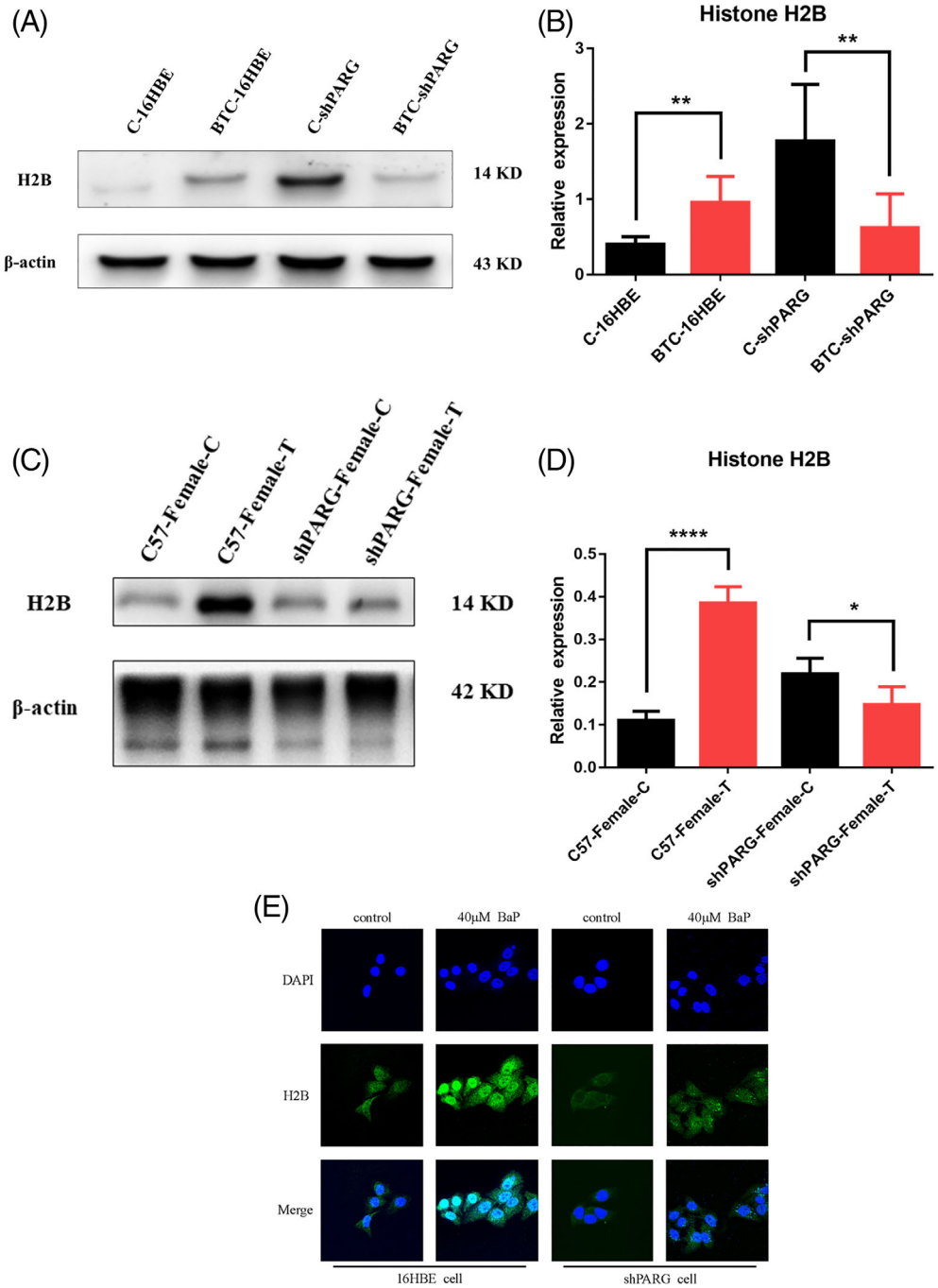

FIGURE 2 Effects of *PARG* on the expression of H2B in BaP-induced carcinogenesis. A, Western blot showing H2B expression in each cell. B,Histogram of the relative expression of H2B in each cell. C,Western blot showing H2B expression in mice. D, Histogram of the relative expression of H2B in each mice. E, Fluorescence intensity of H2B in each cell [Color figure can be viewed at wileyonlinelibrary.com]

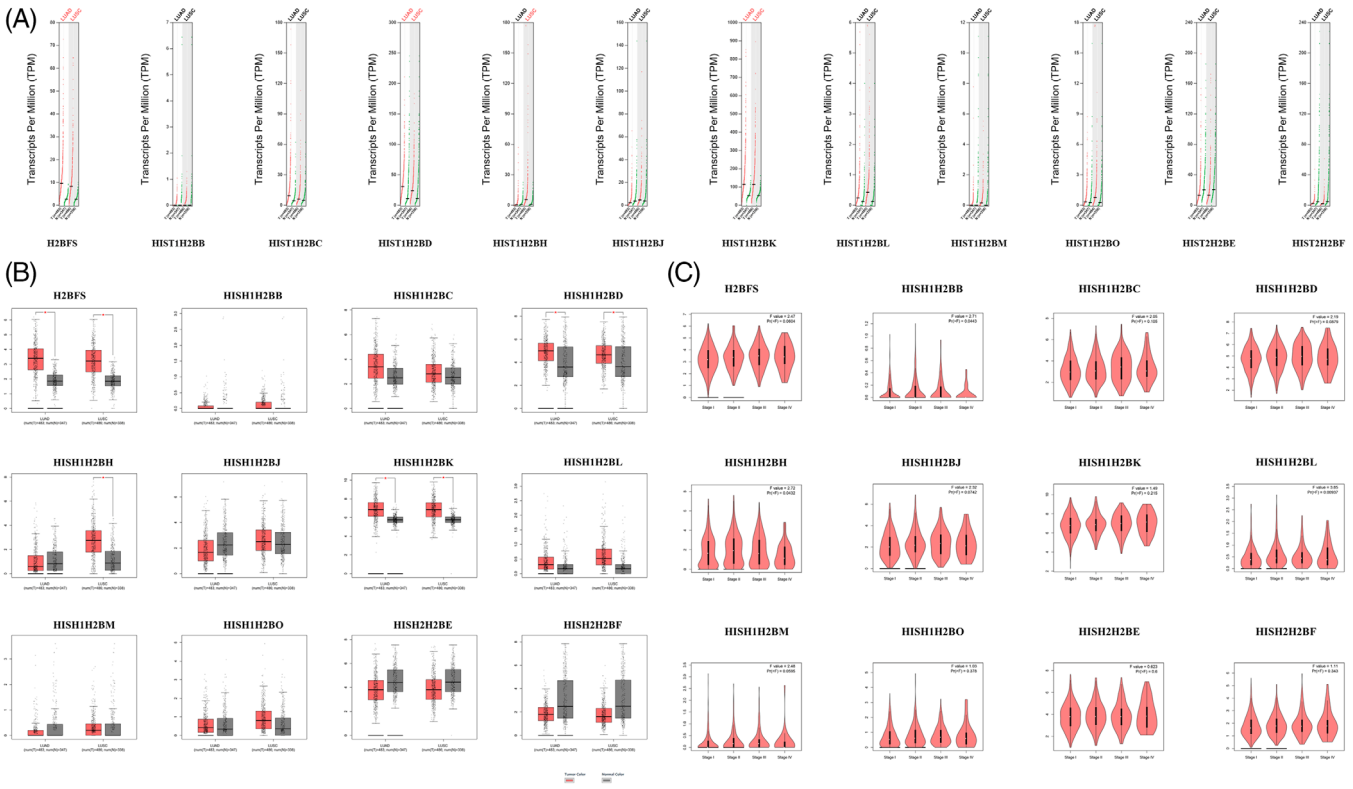

FIGURE 3 Expression of H2B in LC and that of H2B in association with LC tumor stage. A,B, The expression of H2B in LUAC and LUSC. C, The expression of H2B considering the LC tumor stage [Color figure can be viewed at wileyonlinelibrary.com]

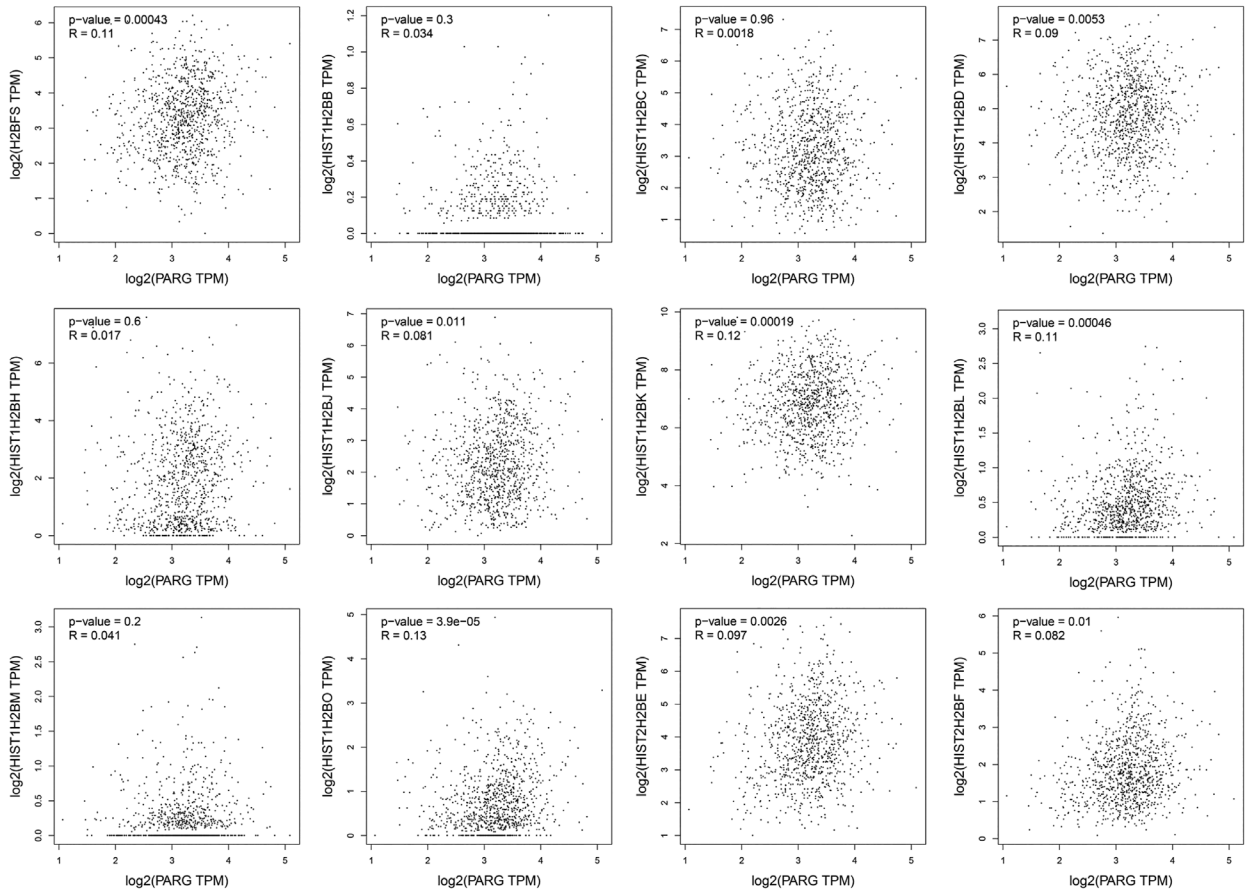

FIGURE 4 Pearson correlation analysis correlation between the expression of H2B subtypes and that of *PARG* in LC tissues

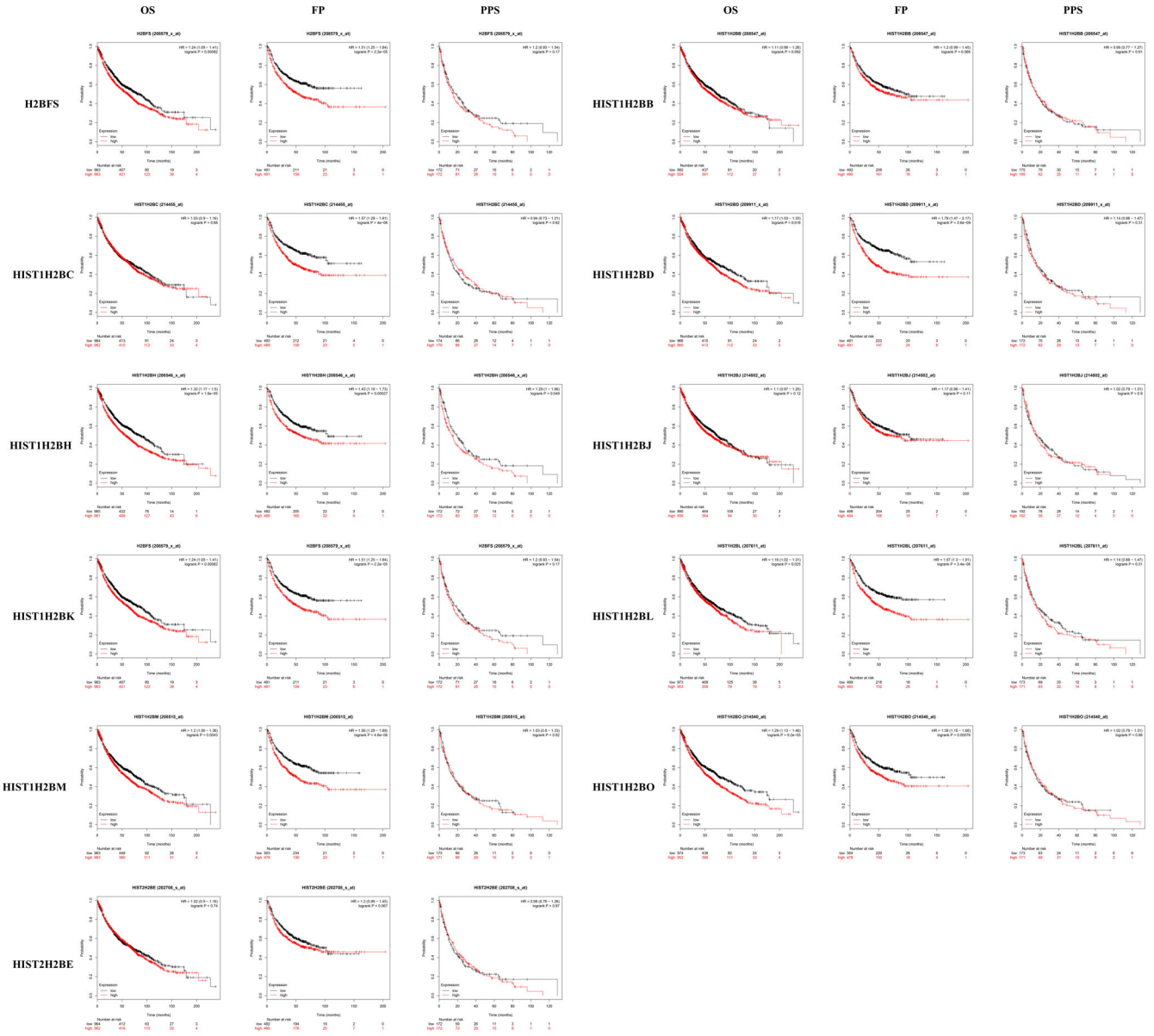

FIGURE 5 Prognostic value of the H2B mRNA level in LC patients. The overall survival (OS), progression-free survival (FP), and postprogression survival (PPS) of all LC patients with respect to H2B expression [Color figure can be viewed at wileyonlinelibrary.com]

indicated that the expression of *H2BFS*, *HIST1H2BD*, and *HIST1H2BK* was higher in LUAD and LUSC tissues than in normal lung tissues, whereas and the expression of *HIST1H2BH* was increased in LUSC tissues than in normal lung tissues (Figure 3A,B). Using the GEPIA2 dataset, we found that the expression of *HIST1H2BB*, *HIST1H2BH*, and *HIST1H2BL* according to the tumor stage of LC varied significantly, whereas the expression of *H2BFS*, *HIST1H2BC*, *HIST1H2BD*, *HIST1H2BJ*, *HIST1H2BK*, *HIST1H2BM*, *HIST2H2BE*, and *HIST2H2BF* according to the tumor stage of LC did not change significantly (Figure 3C). The expression of *H2BFS*, *HIST1H2BD*, *HIST1H2BJ*, *HIST1H2BK*, *HIST1H2BL*, *HIST1H2BO*, *HIST2H2BE*, and *HIST2H2BF* was positively correlated with that of PARG in LC tissues (Figure 4).

3.4 | Correlation between H2B and improved prognosis in cirrhotic patients

We further explored the critical efficiency of H2B in the survival of patients with non-small cell lung cancer. Kaplan-Meier curve analysis and log-rank test revealed that the increased *HIST1H2BH* mRNA level was significantly associated with the OS, FP, and PPS in all the LC

patients ($P < .05$). Increased mRNA levels of *H2BFS*, *HIST1H2BD*, *HIST1H2BK*, *HIST1H2BL*, *HIST1H2BM*, and *HIST1H2BO* were associated with both FP and PPS in all the LC patients ($P < .05$) (Figure 5).

4 | DISCUSSION

A mutation in the H2B gene represents a new class of oncogenic driver.[15] Histones are the basic substrates for chromatin modification and recombinant enzymes, and H2B have been shown to undergo mutation in a variety of tumors.[16] Our previous study showed that *PARG* silencing delay BaP-induced carcinogenesis. The present study is the first to demonstrate the association between *PARG* silencing and H2B downregulation in BaP-induced carcinogenesis. Because of the differences in the sequences and structures of H2B subtypes, we found changes in the expression of H2B subtypes and the modified lineage of H2B after translation. The role of H2B posttranslational modifications in tumorigenesis has been identified. For example, H2BK5ac has been reported to regulate the transformation of epithelial cells into mesenchymal cells.[17] We believe that our findings will contribute to the existing knowledge and provide a theoretical basis for the better prognosis and treatment of LC.

In this study, we found that the levels of several H2B subtypes increased after BaP-induced malignant cell transformation, but *PARG* silencing inhibited this phenomenon. Our in vivo experiments confirmed that *PARG* silencing inhibited BaP-induced malignant transformation by inhibiting the expression of H2B. H2B expression analysis using the online tumor database indicated that the increased expression of *H2BFS*, *HIST1H2BD*, *HIST1H2BH*, and *HIST1H2BK* in LC tissues might play an important role in LC oncogenesis. The transcription products of *H2BFS*, *HIST1H2BD*, *HIST1H2BH*, *HIST1H2BK*, *HIST1H2BL*, *HIST1H2BM*, and *HIST1H2BO* are potential prognostic markers that can be used for improving prognostic accuracy, thereby improving the survival rate of LC patients.

In summary, we have determined here for the first time, that *PARG* silencing reduces BaP-induced carcinogenesis by suppressing H2B expression. This finding provides a theoretical basis of our next study on the role *PARG* silencing in posttranslational modification pedigree changes in H2B in the context of lung tumorigenesis.

ACKNOWLEDGMENTS

Thanks for the support of Natural Science Foundation of Guangdong Province (Project No. 2019A1515011080), Shenzhen Basic Research Project (Project No. JCYJ20190807102803567), Shenzhen Basic Research Discipline Layout (Project no. JCYJ20160328161613864) and Guangdong Medical Science and Technology Research Fund (Project No. A2019554).

ORCID

Zhuoying Zeng https://orcid.org/0000-0001-9727-7994
Desheng Wu https://orcid.org/0000-0002-9058-3793

REFERENCES

1. Ahel I, Ahel D, Matsusaka T, et al. Poly(ADP-ribose)-binding zinc finger motifs in DNA repair/checkpoint proteins. *Nature*. 2008; 451(7174):81-85.
2. Beneke S. Regulation of chromatin structure by poly(ADP-ribosyl) ation. *Front Genet*. 2012;3:169.
3. Huang H, Li X, Hu G, et al. Poly(ADP-ribose) glycohydrolase silencing down-regulates TCTP and Cofilin-1 associated with metastasis in benzo(a)pyrene carcinogenesis. *Am J Cancer Res*. 2015;5(1):155-167.
4. Li X, Li X, Zhu Z, et al. Poly(ADP-ribose) Glycohydrolase (PARG) silencing suppresses Benzo(a)pyrene induced cell transformation. *PLoS One*. 2016;11(3):e0151172.
5. Maselli J, Hales BF, Chan P, Robaire B. Exposure to bleomycin, etoposide, and cis-platinum alters rat sperm chromatin integrity and sperm head protein profile. *Biol Reprod*. 2012;86(5):1-10.
6. Loe-Mie Y, Lepagnol-Bestel AM, Maussion G, et al. SMARCA2 and other genome-wide supported schizophrenia-associated genes: regulation by REST/NRSF, network organization and primate-specific evolution. *Hum Mol Genet*. 2010;19(14):2841-2857.
7. Guo X, Liu W, Pan Y, et al. Homeobox gene IRX1 is a tumor suppressor gene in gastric carcinoma. *Oncogene*. 2010;29(27):3908-3920.
8. Santoro SW, Dulac C. The activity-dependent histone variant H2BE modulates the life span of olfactory neurons. *Elife*. 2012;1:e00070.
9. Beer DG, Kardia SL, Huang CC, et al. Gene-expression profiles predict survival of patients with lung adenocarcinoma. *Nat Med*. 2002;8(8): 816-824.
10. Audia JE, Campbell RM. Histone modifications and cancer. *Cold Spring Harb Perspect Biol*. 2016;8(4):a019521.
11. Esteller M. Cancer epigenomics: DNA methylomes and histone-modification maps. *Nat Rev Genet*. 2007;8(4):286-298.
12. Wang R, Xin M, Li Y, Zhang P, Zhang M. The functions of histone modification enzymes in cancer. *Curr Protein Pept Sci*. 2016;17(5): 438-445.
13. Zeng Z, Liu H, Yuan J, et al. Poly(ADP-ribose) glycohydrolase silencing-mediated maintenance of H2A and downregulation of H2AK9me protect human bronchial epithelial cells from benzo(a) pyrene-induced carcinogenesis. *Toxicol Lett*. 2018;295:270-276.
14. Shechter D, Dormann HL, Allis CD, Hake SB. Extraction, purification and analysis of histones. *Nat Protoc*. 2007;2(6):1445-1457.
15. Bennett RL, Bele A, Small EC, et al. A mutation in histone H2B represents a new class of oncogenic driver. *Cancer Discov*. 2019;9(10): 1438-1451.
16. Nacev BA, Feng L, Bagert JD, et al. The expanding landscape of 'oncohistone' mutations in human cancers. *Nature*. 2019;567(7749): 473-478.
17. Mobley RJ, Abell AN. Controlling epithelial to mesenchymal transition through acetylation of histone H2BK5. *J Nat Sci*. 2017;3(9): e432.

How to cite this article: Zeng Z, Lu J, Wu D, et al. Poly(ADP-ribose) glycohydrolase silencing-mediated H2B expression inhibits benzo(a)pyrene-induced carcinogenesis. *Environmental Toxicology*. 2021;36:291–297. https://doi.org/10.1002/tox.23034